question. This means that a convergent beam is reflected in the same way as from a bent perfect crystal in Johann or Johansson geometry. Usually, the window is wide enough to transmit an energy band that includes both $K\alpha_1$ and $K\alpha_2$ components of the incident beam. The distributions of these components are projected on the (x, x', λ_1) plane in Fig. 7.4.4.3. The sample is placed in the (para)focus of the beam, and often the divergence of the beam is much larger than the width of the rocking curve of the sample crystal. This means that at any given time the signal comes from a small part of the beam, but the whole beam contributes to the background. The profile of the reflection is a convolution of the actual rocking curve with the divergence and wavelength distributions of the beam. The calculated profile in Fig. 7.4.4.2 demonstrates that in a typical case the profile is determined by the instrument, and the peak-to-background ratio is much worse than with a perfect-crystal monochromator.

An alternative arrangement, which has become quite popular in recent years, is one where the plane of diffraction at the monochromator is perpendicular to that at the sample. The beam is limited by slits only in the latter plane, and the wavelength varies in the perpendicular plane. An example of rocking curves measured by this kind of diffractometer is given in Fig. 7.4.4.4. The $K\alpha_1$ and $K\alpha_2$ components are seen separately plus a long tail due to continuum radiation, and the profile is that of the divergence of the beam.

In the Laue method, a well collimated beam of white radiation is reflected by a stationary crystal. The wavelength band reflected by a perfect crystal is indicated in Fig. 7.4.4.1(*b*). The mosaic blocks select a band of wavelengths from the incident beam and the wavelength deviation is related to the angular deviation by $\Delta\lambda/\lambda = \cot\theta\Delta\theta$. The angular resolution is determined by the divergences of the incident beam and the spatial resolution of the detector. The detector is not energy dispersive, so that the background arises from all scattering that reaches the detector. An estimate of the background level involves integrations over the incident spectrum at a fixed scattering angle, weighted by the cross sections of inelastic scattering and the attenuation factors. This calculation is very complicated, but at any rate the background level is far higher than that in a diffraction measurement with a monochromatic incident beam.

7.4.4.3. *Detecting system*

The detecting system is an integral part of the X-ray optics of a diffraction experiment, and it can be included in the phase-space diagrams. In single-crystal diffraction, the detecting system is usually a rectangular slit followed by a photon counter, and the slit is large enough to accept all the reflected beam. The slit can be stationary during the scan (ω scan) or follow the rotation of the sample ($\omega/2\theta$ scan). The included TDS depends on these choices, but otherwise the amount of background is proportional to the area of the receiving slit. It is obvious from a comparison between Fig. 7.4.4.1 and Fig. 7.4.4.3 that a much smaller receiving slit is sufficient in the parallel-beam geometry than in the conventional divergent-beam geometry. Mathieson (1985) has given a thorough analysis of various monochromator–sample–detector combinations and has suggested the use of a two-dimensional $\omega/2\theta$ scan with a narrow receiving slit. This provides a deconvolution of the reflection profile measured with a divergent beam, but the same result with better intensity and resolution is obtained by the parallel-beam techniques.

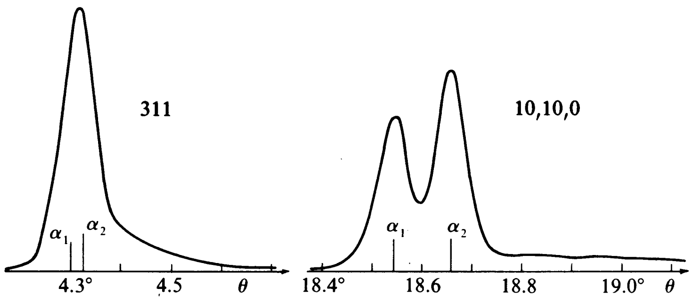

Fig. 7.4.4.4. Two reflections of beryllium acetate measured with Mo$K\alpha$. The graphite (002) monochromator reflects in the vertical plane, while the crystal reflects in the horizontal plane. The equatorial divergence of the beam is 0.8°, FWHM.

The above discussion has concentrated on improving the signal-to-background ratio by optimization of the diffraction geometry. This ratio can be improved substantially by an energy-dispersive detector, but, on the other hand, all detectors have some noise, which increases the background. There have been marked developments in recent years, and traditional technology has been replaced by new constructions. Much of this work has been carried out in synchrotron-radiation laboratories (for

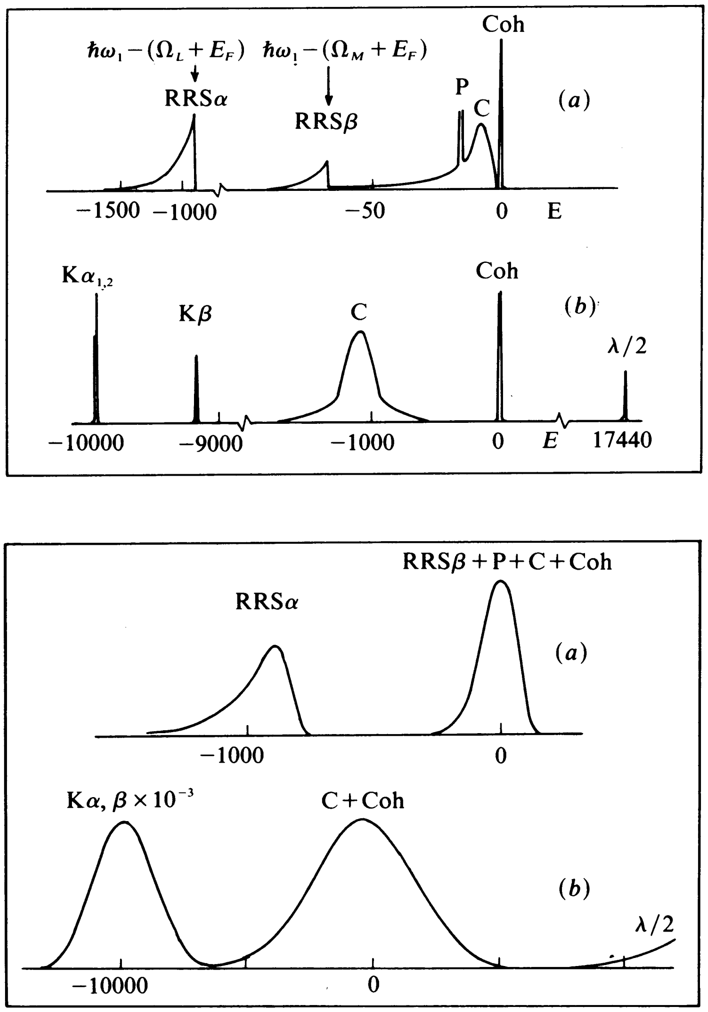

Fig. 7.4.4.5. Components of scattering at small scattering angles when the incident energy is just below the *K* absorption edge of the sample [upper part, (*a*)], and at large scattering angles when the incident energy is about twice the *K*-edge energy [upper part, (*b*)]. The abbreviations indicate resonant Raman scattering (RRS), plasmon (P) and Compton (C) scattering, coherent scattering (Coh) and sample fluorescence ($K\alpha$ and $K\beta$). The lower part shows these components as convoluted by the resolution function of the detector: (*a*) a SSD and (*b*) a scintillation counter (Suortti, 1980).

references